Spin Injection in Thermally Assisted Magnetic Random Access Memory

James G. Deak
NVE Corporation
11409 Valley View Road
Eden Prairie, MN 55344

PACS 02.70.Bf, 05.10.Cc, 05.10.Gg, 07.05.Tp, 85.75.Dd

Abstract - An integrated thermal, micromagnetic, spin-momentum-transfer (SMT) model was developed to study the effect of SMT on the programming current required for thermally assisted magnetic random access memory (MRAM). The thermal portion of the model is used to compute Joule heating by the spin-polarized current, and it is based on a Crank-Nicolson inhomogeneous heat equation solver. The magnetic portion of the model is based on a micromagnetic Langevin dynamic Landau-Lifshitz-Gilbert solver including SMT torque. Simulations of thermally assisted magnetization reversal of 0.09 μm MRAM elements, heated by passing current through the barrier separating the pinned and free layers were performed. The free layer of the MRAM elements was switched using a magnetic field at fixed heating-SMT current bias. Results suggest that a spin-polarized heating current can be used to lower the programming current required to write thermally assisted MRAM if the direction of the heating current is properly synchronized with the reversal field.

One difficulty in developing high-density magnetic random access memory (MRAM) lies in developing a memory element with long data retention time and low error rates that can be programmed with currents that will not damage the MRAM element and can be generated in a practical semiconductor device. These problems result in part from an increasing sensitivity to thermal activation as MRAM is scaled to smaller dimensions reducing the energy required to reverse the memory element. In order to improve stability as MRAM element dimensions are reduced, increases in magnetic anisotropy or magnetic thickness are required. Unfortunately, at small device dimensions these methods increase programming fields and currents to impractical levels.

Methods for writing MRAM using heat in combination with applied magnetic fields or spin momentum transfer (SMT) have previously been described to address this issue. [1] Promising heat-field or magnetothermal (MT) MRAM methods involve the development of new materials with high spin-polarization and low Curie temperature or the use of an additional low Neel temperature antiferromagnet to pin the free layer. SMT-heat methods are also promising, but work needs to be done to develop stable devices that can be written at safe current densities. In spite of the fact that the heat-SMT and MT-MRAM devices have many similarities in their structures, little or no work has been performed to combine the techniques to further reduce programming current. This may in part be because the SMT critical current, I_c, for reversing the magnetization of a mono-domain thin film ferromagnet by SMT in zero temperature simulations is only weakly dependent on magnetic field (H) until H is very near the uniaxial anisotropy field of the film, H_k. [2] In spite of this, it is worth studying the combined effect of H and SMT at elevated temperature, since Joule heating in MT-MRAM devices requires current

densities close to those required for SMT reversal (~10^8A/cm^2), thin ferromagnetic films at ~100 nm dimensions are not strictly mono-domain, and thermal fluctuations in real magnetic layers cause reversal at $H<H_k$ on short time scales. In order to study the possibility of an efficient combined SMT-MT-MRAM, a heat equation solver was developed and integrated with a Langevin dynamic (LD) micromagnetic solver. Simulations of a 130 x90 x 3.6 nm^3 elliptical nickel-iron MRAM cell are presented herein to demonstrate the model.

Micromagnetic models for studying SMT at non-zero temperature exist are often based on the stochastic Landau-Lifshitz-Gilbert (sLLG) equation combined with an additional SMT torque term:

$$\frac{d\hat{m}}{dt} = -\gamma \hat{m} \times \vec{H}_{eff} - \gamma\alpha \hat{\mathrm{m}} \times \left(\hat{\mathrm{m}} \times \vec{H}_{eff}\right) - \gamma \mathrm{J}_{\mathrm{SI}} \hat{\mathrm{m}} \times \left(\hat{\mathrm{m}} \times \hat{\mathrm{m}}_p\right). \qquad (1)$$

Here, the first and second terms on the right hand side are the usual precession and damping terms, and the third term represents SMT from a fixed ferromagnetic layer oriented in direction m_p. "t" is the time, γ the gyromagnetic constant, α the damping parameter, $\hat{m}$ a unit vector representing the direction of magnetization, $J_{SI} = (\eta \hbar i)/(2eM_s V)$, η the spin polarization, M_s the saturation magnetization, V the computational cell volume, and $H_{eff} = H_{exc}+H_d+H_k+H_{ext}+H_I+H_{ns}$, the total local vector magnetic field within the ferromagnetic object due to exchange, demagnetization, anisotropy, external sources, current, and thermal agitation.

Many of the details of the LD micromagnetic solver algorithm used in this work have been previously described. [3] The Gaussian distributed H_{ns} field sequence is calculated using the Box-Müller algorithm, with a standard deviation of

$H_{ns} = \sqrt{2\alpha k_B T/(\gamma Ms V \Delta t)}$ and zero mean. H_I is computed for all current flowing within the mesh using

$$\begin{bmatrix} B_x(\vec{R}_{test}) \\ B_y(\vec{R}_{test}) \\ B_z(\vec{R}_{test}) \end{bmatrix} = \begin{bmatrix} 0 & \Delta z F(\Delta x, -\Delta z, \Delta y, L_y) & -\Delta y F(\Delta x, \Delta y, \Delta z, L_z) \\ -\Delta z F(-\Delta z, \Delta y, \Delta x, L_x) & 0 & \Delta x F(\Delta x, \Delta y, \Delta z, L_z) \\ \Delta y F(-\Delta z, \Delta y, \Delta x, L_x) & -\Delta x F(\Delta x, -\Delta z, \Delta y, L_y) & 0 \end{bmatrix} \begin{bmatrix} I_x(\vec{R}_{source}) \\ I_y(\vec{R}_{source}) \\ I_z(\vec{R}_{source}) \end{bmatrix} \quad (2a)$$

$$F(a,b,c,L) = \frac{10^{-7}}{a^2+b^2}\left\{\frac{L/2-c}{\sqrt{a^2+b^2+(L/2-c)^2}} + \frac{L/2+c}{\sqrt{a^2+b^2+(L/2+c)^2}}\right\}. \quad (2b)$$

In this notation, "test" indicates the point where the B field from a current filament of length $L = \sqrt{L_x^2 + L_y^2 + L_z^2}$ at the "source" point is computed. Thus, $\vec{R}_{test} = x_{test}\hat{x} + y_{test}\hat{y} + z_{test}\hat{z}$ and $\vec{R}_{source} = x_{source}\hat{x} + y_{source}\hat{y} + z_{source}\hat{z}$. The deltas are $\Delta x = x_{test} - x_{source}$, $\Delta y = y_{test} - y_{source}$, and $\Delta z = z_{test} - z_{source}$.

The $\hat{m}\times(\hat{m}\times\hat{m}_p)$ representation of the SMT torque is probably the most commonly accepted form. [4] Addition of this term to equation 1 has an interesting consequence in that it produces a current and magnetization orientation dependent change in the effective damping parameter of the material. [5] Consider the case where m_p is parallel to H_{eff}. In this case, the sLLG equation can be rewritten as $\frac{d\hat{m}}{dt} = -\gamma\hat{m}\times\vec{H}_{eff} - \gamma\tilde{\alpha}\hat{m}\times(\hat{m}\times\vec{H}_{eff})$ with $\tilde{\alpha} = a \pm J_{SI}/H_{eff}$. SMT torque changes the effective damping causing magnetic excitations to damp out more slowly or quickly in time, depending on the orientation of m_p. The α value in the thermal H_{ns} term is not rescaled. The difference between the damping in the deterministic and stochastic portions of the SMT modified sLLG equation implies that SMT torque should change the effective magnetic temperature of the sample to $\tilde{T} = (\alpha/\tilde{\alpha})T$, when the spin polarization of the current is collinear with the magnetization of the free layer. Using switching

measurements, it is difficult to separate $\widetilde{T}$ from a lowering of the energy barrier, ΔE, since the measurements are dependent on the ratio $\Delta E/k_B T$. In any case, the effective increase in $\widetilde{T}$ or lowering of ΔE, should facilitate magnetic reversal at lower H or T. This work thus focuses on reducing the programming current of MT-MRAM and through the use of SMT.

Heat flow due to Joule heating at the tunnel barrier is simulated using the heat equation modified for use in nonuniform materials and to include temperature dependent material parameters:

$$\rho_m(x,y,z)C_p(x,y,z)\frac{\partial T(x,y,z)}{\partial t} = \vec{\nabla}\cdot\left[k(x,y,z)\vec{\nabla}T(x,y,z)\right] + g(x,y,z,T,t) \quad (3)$$

Here, ρ_m is the local density, C_p the local heat capacity, T the local temperature, k the local thermal conductivity, and g(x,y,z,T,t) is the time and temperature dependent local power generation in the simulated device. For Joule heating in materials with temperature dependent resistivity, the power generation term is expressed as

$$g(x,y,z,T,t) = J^2(x,y,z,t)\rho(x,y,z,T), \quad (4)$$

where the local current density, J, is dependent on time, and the local resistivity, ρ, is dependent on temperature. Equation 3 was discretized using a Crank-Nicolson finite-difference approach. The resulting set of matrix equations are efficiently solved in 3D using a sparse-matrix preconditioned successive-over-relaxation solver

The integrated thermal-micromagnetic-SMT simulation method is outlined in Figure 1. Note that the block labeled "RG Scaling" indicates that renormalization group scaling of the micromagnetic simulation input parameters is applied to account for errors

resulting from truncation of short wavelength excitations in the simulated spin lattice due to the coarse grained mesh (5 x 5 x 3.6 nm^3). [6]

A cross-section of the simulated MRAM element is shown in Figure 2. The device sandwiches a free layer between two oppositely oriented pinned layers. The free layer is separated from one pinned layer by an AlOx (tunnel barrier) spacer and from the other by a Cu spacer. Since the AlOx barrier magnetoresistance is much greater than that of the Cu spacer, this structure can have a large magnetoresistance. The oppositely oriented pinned layers effectively double the spin polarization in the free layer since across one spacer, spin polarized electrons are reflected and those across the other are transmitted. In order to simulate this stack, an effective η=0.9 was thus used. Thermal parameters and geometry used for simulation are listed in Table 1. The free layer is composed of permalloy, M_s = 8x10^5 A/m, A = 1e-11 J/m, α = 0.02, and T_c = 850 K. The tunnel barrier has a resistivity of ~5 $\Omega\mu m^2$, which assuming a 200 mV reliability threshold, safely permits about 300 μA of current.

Joule heating results are shown in Figure 3. The free layer temperature is uniform to better than 1%. The average temperature is thus used for the micromagnetic simulation. Micromagnetic simulation results are shown in Figure 4. The combination of applied field, SMT, and temperature sufficiently lower ΔE so that the sense layer magnetization reverses within the write cycle. Figure 4(A) shows that increased temperature strengthens the dependence of the SMT I_c on H and decreases the SMT I_c value. Figures 4(B)-4(D) show that at low I_{wrt} neither H nor H combined with SMT can reverse the bit. At intermediate I_{wrt}, only SMT - H can program the bit, and at higher I_{wrt}, H alone can be used to program the bit. For the present work, tunneling hotspots through

the barrier were also considered. Simulations restricting tunnel current to an area of about 10% of the AlOx spacer show more than a 50% reduction in SMT I_c.

LD micromagnetic simulation suggests that increasing temperature increases the dependence of SMT on applied field. A method for writing an MRAM element utilizing a combination of SMT, heat, and applied field has thus been suggested. SMT and applied magnetic field allow thermally assisted writing of an MRAM element without the need to heat the free layer above its T_c at currents lower than needed if only Joule heating and H were used to overcome ΔE. Switching speed was found to range from 5 ns at 327 μA to greater than 50 ns at 150 μA. For the particular geometry and set of materials studied, the use of SMT provides roughly a 15% reduction in write current. Simulation including tunneling hotspots at 10% of the total junction area shows switching at less than 150 μA, and can potentially reduce the write current by 50% below the uniform current simulation results. Further simulations have shown that decreasing the T_c of the free layer to 500 K allows a device of the same dimensions to be built that could be written at less than 100 μA through the memory element, in spite of the fact that 100 μA only provides about 50 K of heating.

ACKNOWLEDGEMENT - This work was funded in part by DARPA and MDA.

References

[1] J. M. Daughton, A. V. Pohm, and M. C. Tondra, U. S. Patent No. 6,744,086 B2 (1 June 2004); J. M. Daughton, Spintronics applications at NVE, presented at First Annual CNS Nanotechnology Symposium, Cornell University, Ithaca, NY, May 14, 2004.

[2] J. Z. Sun, Phys. Rev. B 62, 570 (2000).

[3] R. H. Koch, J. A. Katine, and J. Z. Sun, Phys. Rev. Lett. 92, 088302-1 (2004); S. Li and S. Zhang, Phys. Rev. B 69, 134416 (2004).

[4] J. L. Garcia-Palacios and F. J. Lazaro, Phys. Rev. B 58(22), 14937 (1998); J. G. Deak, J. Appl. Phys. 93(10), 6814 (2003).

[5] J. Slonczewski, J. Magn. Magn. Mater. 159, L1 (1996).

[6] G. Grinstein and R. H. Koch, Phys. Rev. Lett. 90(20), 207201-1 (2003).

Figures

Figure 1. Integrated micromagnetic-thermal-SMT simulation method.

Figure 2. Simulated MRAM element. TV = thermal via, I_H = current used to produce the write field, FM-clad = ferromagnetic cladding, I_{wrt} = write current, and I_{rd} = read current. The bit is written by passing current I_H through the write conductor and tapping some current through the bottom TV to produce SMT and heat. The direction of I_{wrt} must be synchronized with I_H.

Figure 3. (a) Temperature as a function of time and current, and the input write current waveform. (b) Temperature distribution in the plane of the free layer 20 ns after applying 175 μA. The contours are spaced 10 K apart, and the average temperature of the free layer is 456.5 K±2K.

Figure 4. (A) Average SMT switching current computed at fixed H and T with $\eta = 0.45$. (B)-(D) show the benefit of including SMT plus Joule heating in the MT-MRAM device at write currents ranging from 150 μA (B) to 200 μA (D). SMT reduces the write current by about 25 μA. Inset of (B) shows SMT switching at 150 μA with 10% area tunneling hotspot.

Table 1. Thermal simulation parameters for the model MRAM bit. Simulated thermal resistance between FM-FREE and CMOS is 3.6e6 K/W. The substrate and top conductor are assumed to be a constant heat bath at 300. Neumann boundaries are assigned to the vertical edges of the simulated volume.

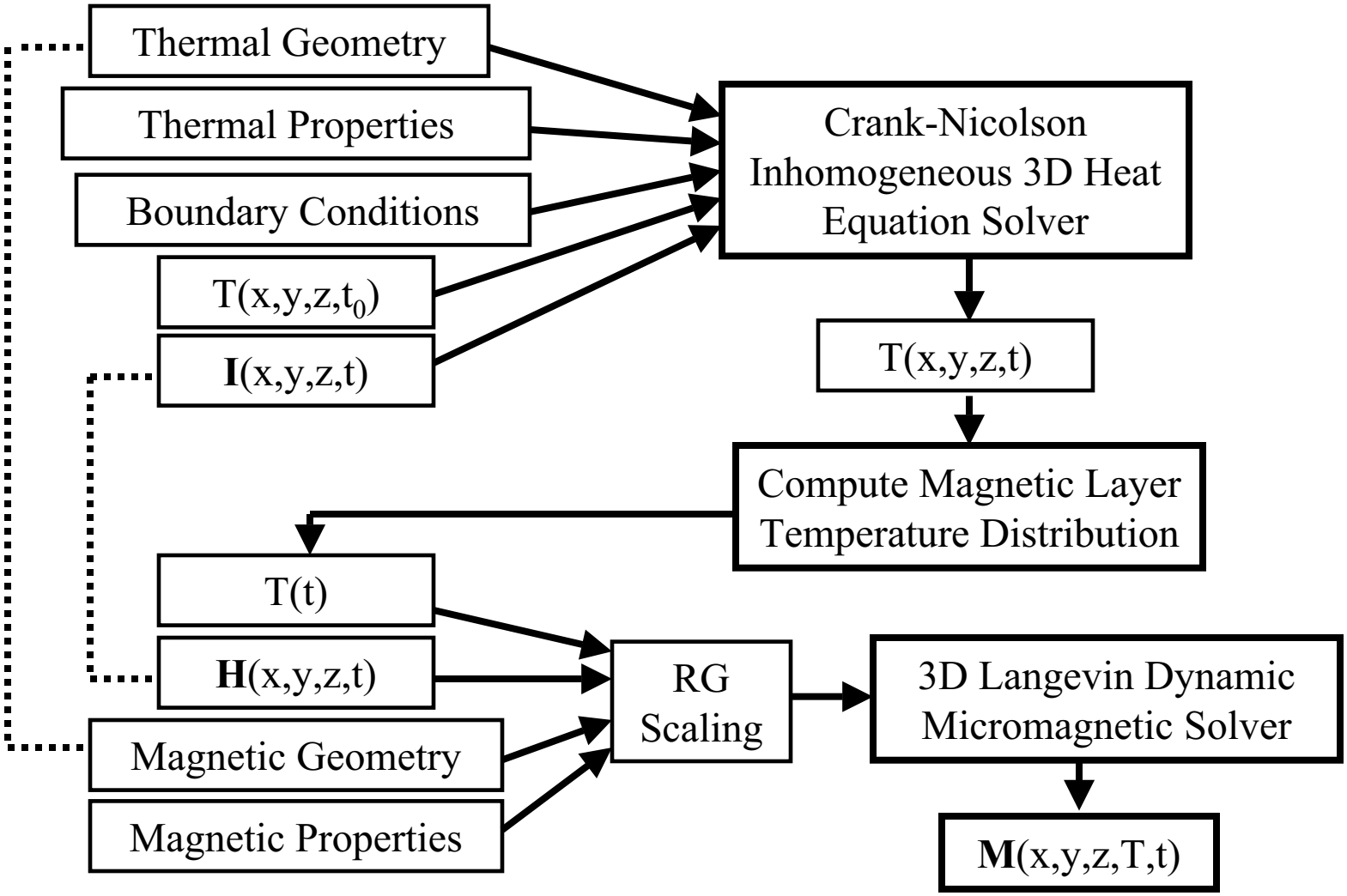
Thermal Geometry
Thermal Properties
Boundary Conditions
T(x,y,z,t0)
I(x,y,z,t)
Crank-Nicolson Inhomogeneous 3D Heat Equation Solver
T(x,y,z,t)
Compute Magnetic Layer Temperature Distribution
T(t)
H(x,y,z,t)
Magnetic Geometry
Magnetic Properties
RG Scaling
3D Langevin Dynamic Micromagnetic Solver
M(x,y,z,T,t)

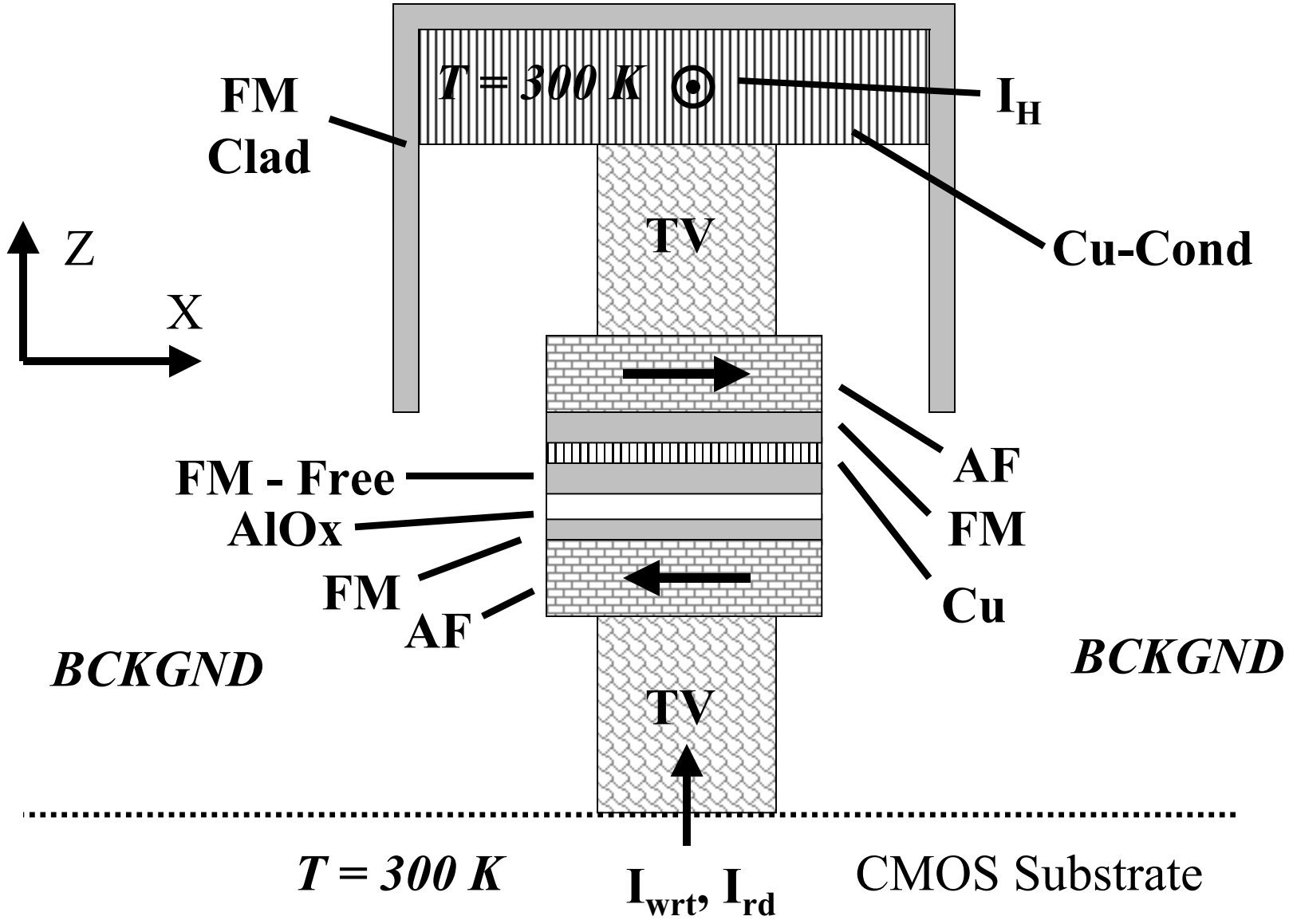
FM
Clad
T = 300 K
I_H
TV
Cu-Cond
Z
X
FM - Free
AlOx
FM
AF
AF
FM
Cu
BCKGND
BCKGND
TV
T = 300 K
I_wrt, I_rd
CMOS Substrate

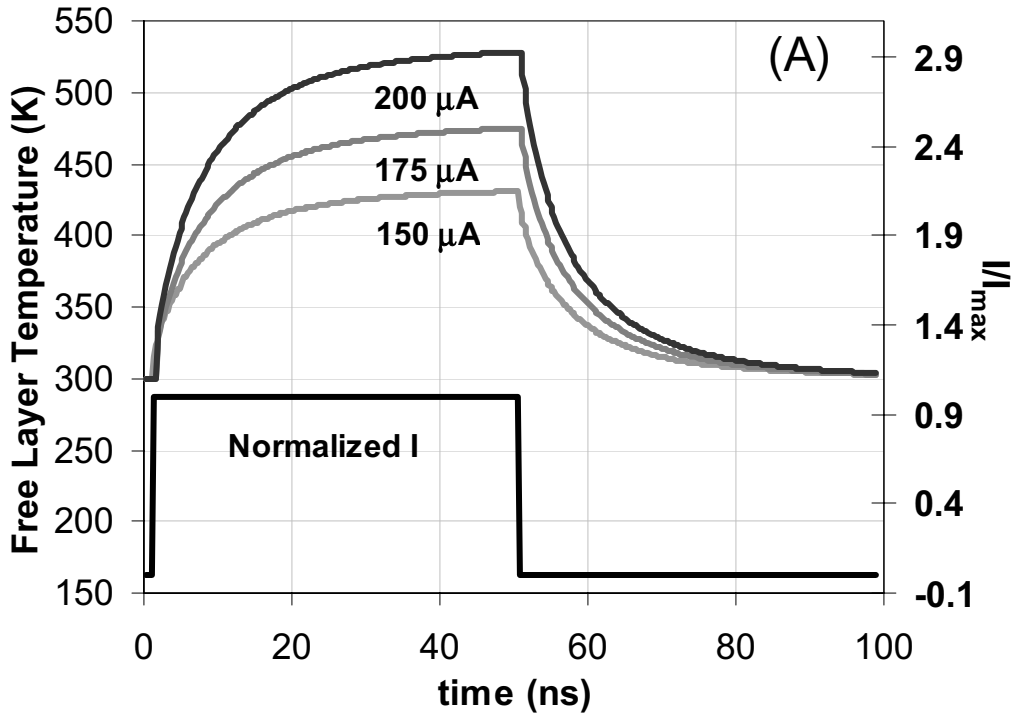
(A)
Free Layer Temperature (K)
550
500
450
400
350
300
250
200
150
200 μA
175 μA
150 μA
Normalized I
2.9
2.4
1.9
1.4
0.9
0.4
-0.1
I/I_max
0
20
40
60
80
100
time (ns)

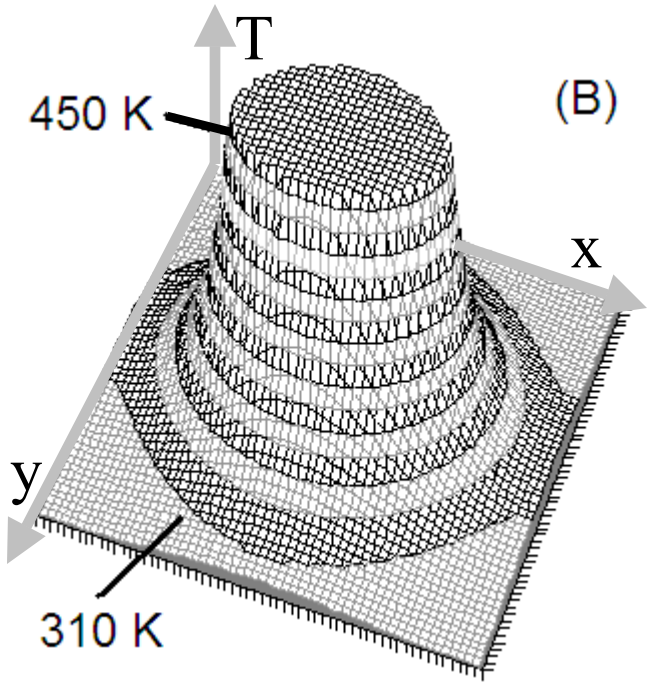
T
450 K
(B)
x
y
310 K

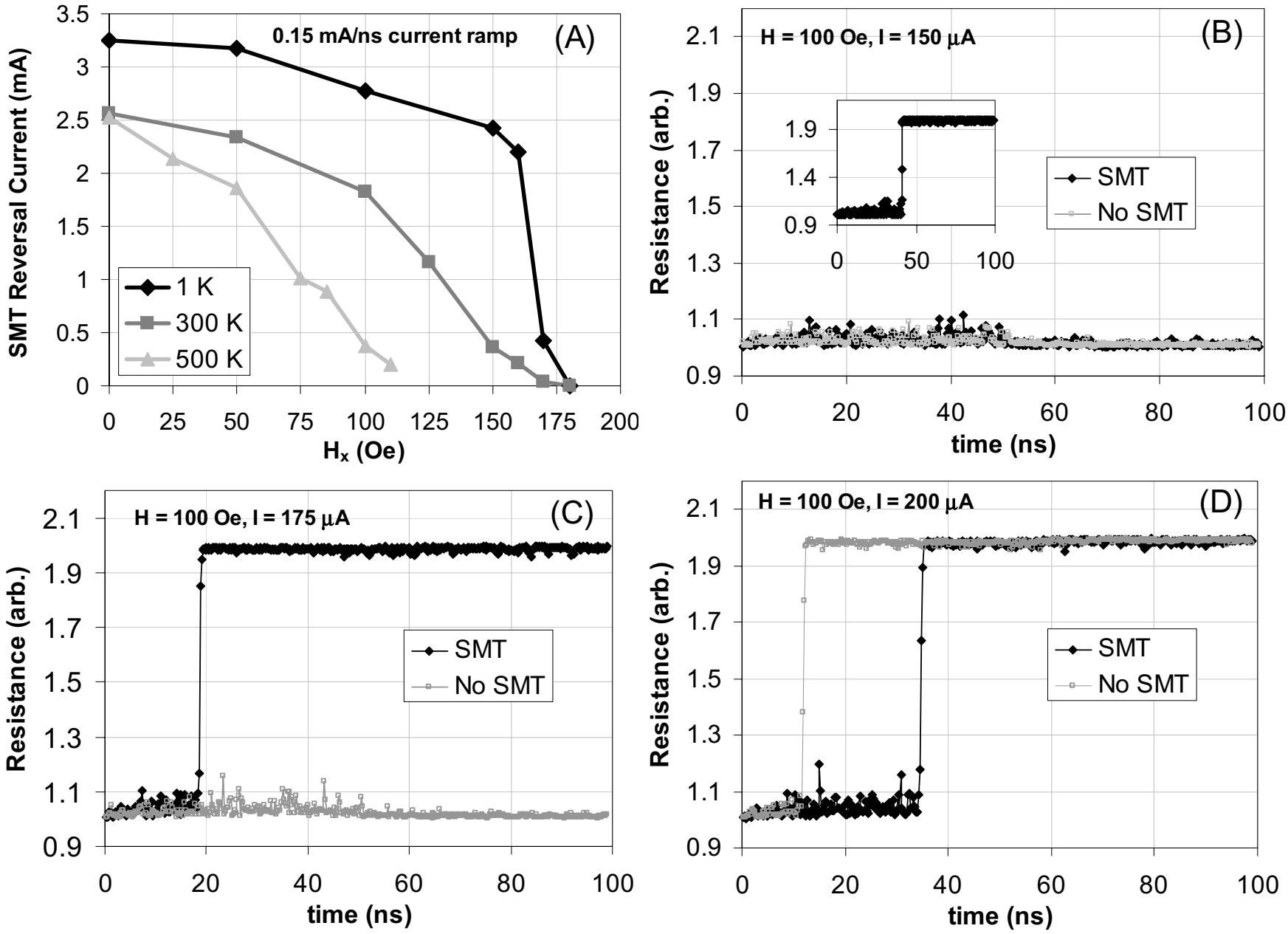
0.15 mA/ns current ramp
(A)
SMT Reversal Current (mA)
H_x (Oe)
1 K
300 K
500 K
H = 100 Oe, I = 150 μA
(B)
Resistance (arb.)
time (ns)
SMT
No SMT
H = 100 Oe, I = 175 μA
(C)
H = 100 Oe, I = 200 μA
(D)

	BCKGND	TV	AF	FM	AlOx	FM-Free	Cu	FM	AF	TV	units
K	0.003	0.014	0.010	0.197	0.014	0.197	4.010	0.197	0.010	0.014	W/cm-K
DENS	2.200	2.200	12.000	8.700	2.200	8.700	8.930	8.700	12.000	2.200	g/cc
C	1.050	1.050	0.277	0.500	1.050	0.500	0.385	0.500	0.277	1.050	J/g-K
RHO	1.00E+02	1.00E-03	1.00E-03	1.00E-04	7.16E-01	1.00E-04	1.70E-06	1.00E-04	1.00E-03	1.00E-03	ohm-cm
LX	300	51	130	130	130	130	130	130	130	51	nm
LY	300	51	90	90	90	90	90	90	90	51	nm
Lz	156	64	8	4	2	4	2	4	8	60	nm
Level	0	0	64	72	76	78	82	84	88	96	nm
SHAPE	Rect	Ellipse	Ellipse	Ellipse	Ellipse	Ellipse	Ellipse	Ellipse	Ellipse	Ellipse	char